Inactivation of the cardiac Na^+ channels in guinea-pig ventricular cells through the open state

Tamotsu Mitsuiye and Akinori Noma

Department of Physiology, Faculty of Medicine, Kyoto University, Sakyo-ku, 606 Kyoto, Japan

1. The inactivation kinetics of the Na^+ current were investigated using the improved oil-gap voltage clamp method in single ventricular cells of guinea-pig hearts.

2. Activation of the Na^+ current was observed on depolarization more positive than −50 mV from a holding potential of −100 mV, and inactivation was complete during these depolarizations. The time course of current decay was fitted by a double exponential at potentials between −40 and −15 mV, and virtually by a single exponential at more positive potentials. The decay time courses examined either by the double-pulse protocol or the single-pulse protocol were similar.

3. The double-pulse protocol clearly revealed a sigmoidal onset of inactivation on depolarization. The initial delay of inactivation decreased with more positive potentials. The time course of double-pulse inactivation was reconstructed by integrating the Na^+ current recorded by a continuous depolarization.

4. These findings are consistent with the hypothesis that the cardiac Na^+ channel inactivates exclusively through the open state.

A fast voltage clamp using the improved oil-gap method revealed that the activation time course of the cardiac Na^+ current is virtually a single exponential in cardiac ventricular cells (Mitsuiye & Noma, 1992, 1993), in contrast to the sigmoidal onset of activation so far described. The present study uses the same technique, and aims to characterize the inactivation of cardiac Na^+ channels. Inactivation kinetics of the Na^+ channel are still controversial. In recent studies, a significant fraction of the channels were considered to inactivate from a closed state over the range of potentials of activation in guinea-pig ventricular cells and canine Purkinje cells (Yue, Lawrence & Marban, 1989; Scanley, Hanck, Chay & Fozzard, 1990), or at least at potentials of partial activation in canine ventricular myocytes (Berman, Camardo, Robinson & Siegelbaum, 1989). On the other hand, Benndorf & Nilius (1987) observed a delay of inactivation after depolarization during whole-cell recordings in mouse ventricular cells. Similarly, Mitsuiye & Noma (1987*b*, 1989) observed a delay of inactivation in preliminary studies using the oil-gap method in guinea-pig ventricular cells. Our single-channel analysis also suggested a delay of inactivation (Kimitsuki, Mitsuiye & Noma, 1990*a*).

The present study addresses the question of whether the cardiac Na^+ channel inactivates through the open state. It is essential to use the double-pulse protocol (experiments in nerve: Bezanilla & Armstrong, 1977; Gillespie & Meves, 1980; Nonner, 1980; Goldman & Kenyon, 1982), which requires fast and adequate voltage control (Gillespie & Meves, 1980). We used the improved oil-gap method and examined whether the availability of the cardiac Na^+ channels decreases with a distinct delay after depolarization. We provide several lines of experimental evidence showing that inactivation from a closed state is negligible in cardiac Na^+ channels at potentials where macroscopic Na^+ channel activation was obvious.

METHODS

Preparation

The heart was dissected out from the guinea-pig under deep pentobarbitone (50 mg kg^{-1}) anaesthesia. Single myocytes were obtained from the ventricles using the collagenase method essentially as originally described (Powell, Terrar & Twist, 1980; Isenberg & Klöckner, 1982).

Oil-gap voltage clamp and data analysis

Details of the voltage clamp method for single ventricular myocytes using an oil-gap have been described previously (Mitsuiye & Noma, 1992; see also Mitsuiye & Noma, 1987). In brief, a single ventricular cell was stretched between the external and internal solution compartments across an oil-gap 30–40 μm in width. The end of the cell in the internal solution was ruptured by the tip of a glass pipette and the current through the cell membrane exposed to the external solution was recorded

through the oil-gap. A seal resistance (R_s) of greater than 1 GΩ in the oil-gap facilitated the compensation of series resistance to less than 50 kΩ. The peak amplitude of the Na^+ current was reduced to less than 30 nA by reducing the membrane area exposed to the external solution (140 mM Na^+). Currents in response to small hyperpolarizing voltage steps (10–20 mV; $n = 10$–40) from −100 mV were averaged and scaled for subtraction of both capacitive (I_{cap}) and leak current (I_{leak}), except in the measurement of the Na^+ channel availability using the double-pulse protocol. The electrical circuit of the home-made amplifier, and data analysis were the same as in the previous study (Mitsuiye & Noma, 1992). Curve-fitting to a current recording or to the envelope of peak Na^+ current was made using the least-squares algorithm (pattern search method: Colquhoun, 1971). The data are expressed as means ± S.D. (n = number of experiments) whenever possible. Statistical significance between two groups of data was determined using Student's t test, if necessary.

Solutions

The compositions of internal and external solutions were the same as those used in the previous study (Mitsuiye & Noma, 1992). The external solution contained (mM): 140 NaCl, 5·4 CsCl, 0·5 $MgCl_2$, 1·8 $CaCl_2$ and 11 glucose; pH was adjusted to 7·4 with 5 mM Hepes–NaOH. The internal solution contained (mM): 105 caesium aspartate, 0·5 $MgCl_2$, 10·0 NaCl, 5·0 K_2ATP and 5·0 EGTA; pH was adjusted to 7·2 with 5 mM Hepes–CsOH. All experiments were carried out at room temperature (19 ± 1 °C).

RESULTS

Time course of decay of the cardiac Na^+ current during depolarization

The Na^+ current was recorded by depolarizing the membrane from −100 mV, and linear capacitive and leak currents were subtracted (Mitsuiye & Noma, 1992). Figure 1 shows a representative family of Na^+ currents. Steady current levels at 200 ms after depolarization were zero in all recordings. The time course of current decay was fitted with a sum of two exponentials using the least-squares routine (Colquhoun, 1971). At membrane potentials of −40 (*a*), −35 (*b*) and −30 mV (*c*), the current decay was very slow and the use of longer pulse durations (*a′*–*c′*, 200 ms) was essential to define the slow component with reference to the zero-current level. The two exponential components were well separated in the Na^+ current inactivation at potentials negative to −15 mV. At more positive potentials, the two time constants of the fitted curve were almost identical, and therefore the decay was re-evaluated by fitting a single exponential.

The mean of the time constants for both the fast and slow components of inactivation are plotted against membrane potential in Fig. 2. It is evident that the magnitude of the time constant decreased with more positive potentials over

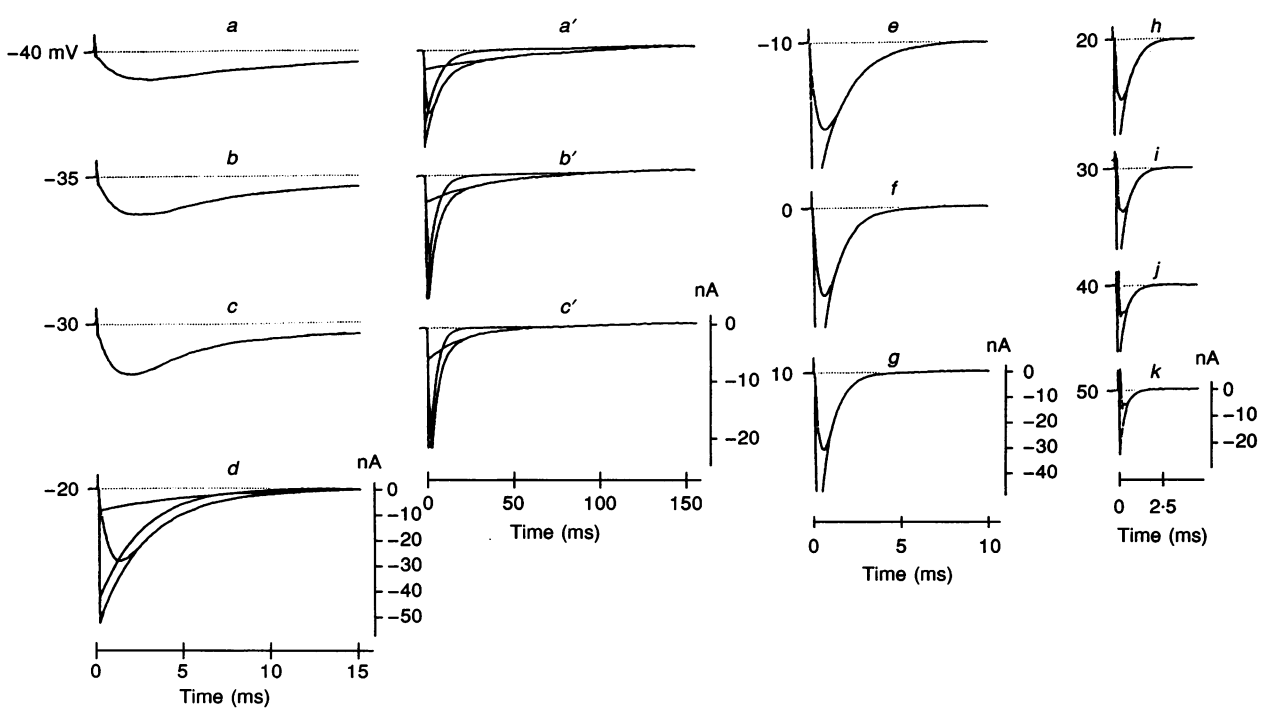

Figure 1. Time course of decay of cardiac Na^+ current recorded by the oil-gap method

The Na^+ current was recorded by depolarizing to potentials indicated, from a holding potential of −100 mV. Linear leak and capacitive currents were subtracted. Records in *a′*–*c′* are shown on a slower time scale and with a higher magnification than in *a*–*c*. The current records in *d* and *a′*–*c′* were fitted by the sum of two exponentials, which are also illustrated. The records in *e*–*k* were fitted with a single exponential curve.

the entire potential range examined. In this semi-logarithmic plot, the relationship was almost linear over the potential range positive to +10 mV. The time constants at negative potentials deviated from this linear relationship and showed higher voltage dependency. The line in Fig. 2 is given by:

$$\tau(V) = \tau(0) \exp(-V/s) \quad (1)$$

where $\tau(V)$ indicates the time constant (ms) at potential V, and s is the slope factor. The value of $\tau(0)$ was 0·962 ± 0·033 ms and s was 44·7 ± 1·1 mV ($n = 9$).

Initial delay of inactivation measured by the double-pulse protocol

Inactivation exclusively through the open state of the Na^+ channel should show a delay before the full activation of the Na^+ current. This delay of inactivation was analysed by the double-pulse protocol (Hodgkin & Huxley, 1952), in which the Na^+ current peak amplitude is measured during a constant second pulse (test pulse) applied immediately after interrupting, at different times, the first depolarizing pulse (conditioning pulse). So that the normalized peak amplitudes of the current during the test pulse correctly reflect the availability of Na^+ channels (Gillespie & Meves, 1980), the test pulse must be separated from the conditioning pulse by a brief repolarization, to reset the activation parameter.

We first determined the appropriate length of gap. Original currents at the test pulse are shown for each experiment in the inset of Fig. 3, where the currents shown on the left are those obtained with conditioning pulses (−10 mV) shorter than 1 ms, and those shown on the right with pulses longer than 1 ms. If the test pulse was not separated from the conditioning pulse (Fig. 3*A*), the peak time of the Na^+ current of the test pulse was progressively shortened as the conditioning pulse was prolonged. The peak time became constant when the test pulse was separated from the conditioning pulse by a repolarization of 1 or 2 ms to −100 mV (Fig. 3*B* and *C*). The normalized amplitudes of the peak Na^+ current are plotted against the duration of the conditioning pulse in Fig. 3*A*, *B* and *C*. We conclude that the decay time course of availability obtained with a gap of 1 ms is valid, whereas the relatively long delay and the slow time course in Fig. 3*A* is affected by the variable magnitude of the activation parameter at the peak time of the Na^+ current.

In Fig. 3, the arrow on the ordinate of each graph indicates the relative amplitude of test pulse current, recorded after sufficiently long conditioning pulses for inactivation to reach a steady state. Since the Na^+ current was completely inactivated during the preceding pulse, the residual Na^+ current may be due to a removal of inactivation at −100 mV during the short gap (Fig. 3*A*). If so, the normalized amplitude of the test pulse Na^+ current (availability, $A'(t)$) will be determined by the sum of two fractions; one is the fraction of channels remaining available at the end of the conditioning pulse of duration t ($A(t)$), and the other is the fraction of channels which recovered from inactivation during the gap:

$$A'(t) = A(t) + P_r(1 - A(t)), \quad (2)$$

where P_r indicates the proportion of the channels which recovered from inactivation during the gap and is a function of both the potential and the length of the gap.

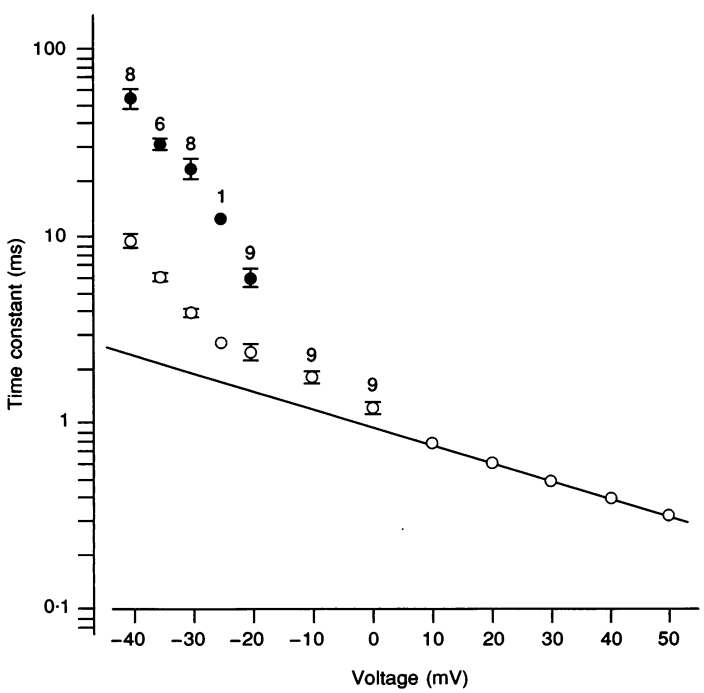

Figure 2. Semi-logarithmic plots of time constants of the Na^+ current decay

Means ± S.D. of time constants of the slow component (●) and the fast component (○) at potentials more negative than −15 mV. The numbers indicate the number of experiments. All the symbols at > −15 mV are those of single exponential decays from nine experiments. The line is drawn using eqn (1):

$$\tau(V) = 0{\cdot}962 \exp(-V/44{\cdot}7).$$

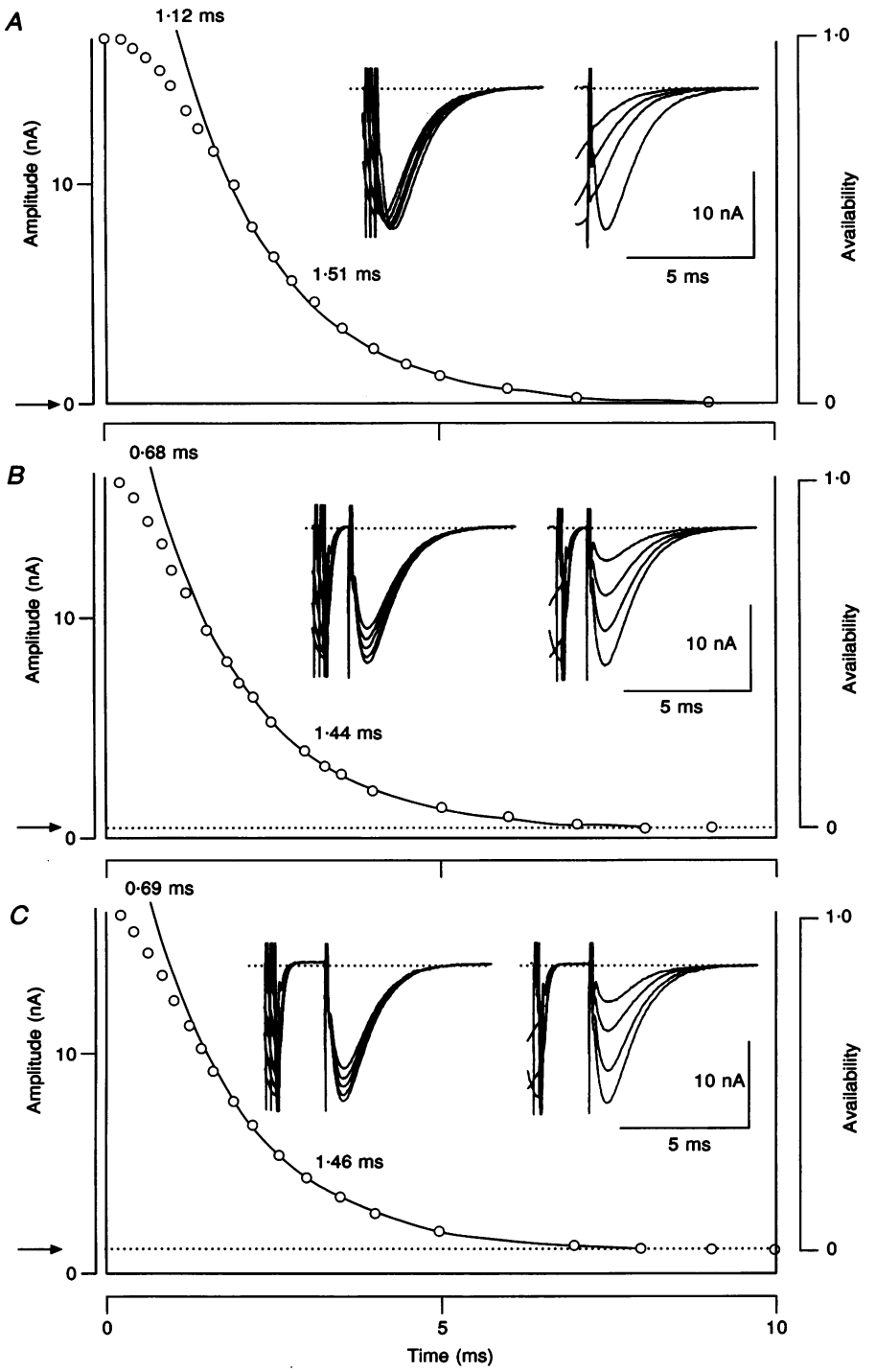

Figure 3. Measurements of channel availability with gaps of 0 (*A*), 1 (*B*) and 2 ms (*C*) between the conditioning pulse and the test pulse

The holding potential and the gap potential were −100 mV, and membrane potentials of both the conditioning and test pulses were −10 mV. The duration of the conditioning pulse was varied and peak amplitudes of the Na^+ current were plotted. Insets: superimposition of the original current records obtained with conditioning pulses shorter than 1 ms (left-hand panel), and with longer conditioning pulses (right-hand panel). The top of the frame gives the maximum amplitude of the peak Na^+ current without conditioning pulse. The curves are the fit of a single exponential and their time constants are shown. The time of intersection of the fitted exponential curve with the maximum amplitude is indicated. The arrow on the left-hand *Y*-axis indicates the amplitude of Na^+ current at test pulse when the conditioning pulse was sufficiently long, and the right-hand *Y*-axis indicates the availability of the Na^+ channels.

Thus the availability at the end of the conditioning pulse is given by:

$$A(t) = (A'(t) - P_r)/(1 - P_r). \quad (3)$$

Since the Na^+ channel is almost completely inactivated ($A(t) = 0$) during a sufficiently long depolarization (Fig. 1), the value of P_r (arrow in Fig. 3) is given by the relative amplitude of the Na^+ current recorded after sufficiently long conditioning pulses. The scale shown to the right of graphs *B* and *C* in Fig. 3 indicates the magnitude of $A(t)$.

In the following measurements, the test pulse of the double-pulse protocol was fixed at −10 mV, and 20 ms in duration; the gap interval was 1 ms. The pair of conditioning and test pulses were separated by an interval longer than 2 s. The control Na^+ current was obtained by

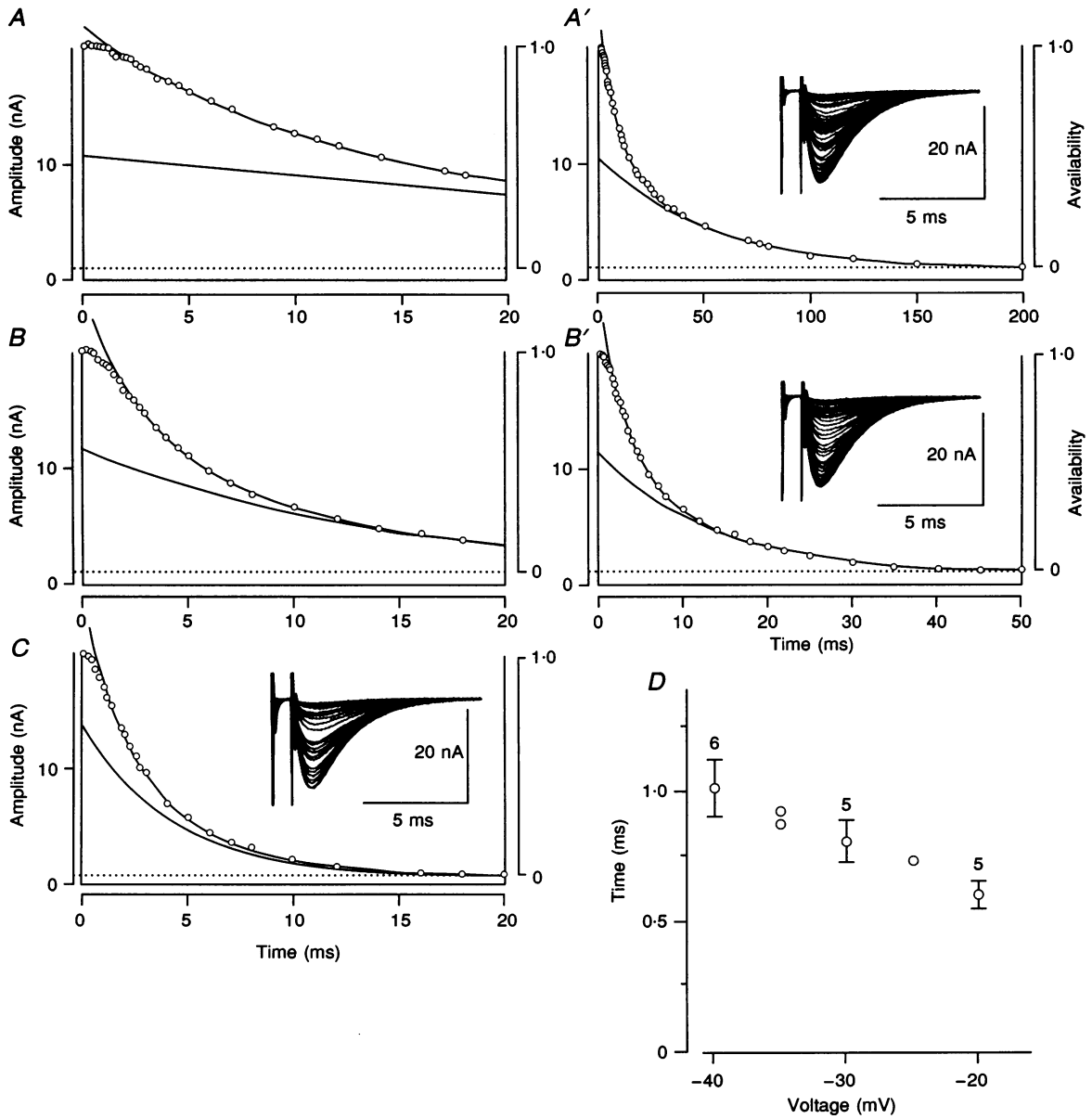

Figure 4. Measurement of channel availability using conditioning pulses to −40 (*A*, *A′*), −30 (*B*, *B′*) and −20 mV (*C*)

The test potential was −10 mV, and holding potential −100 mV. The original Na^+ currents at the test pulse are superimposed in the insets. The time courses at −40 and −30 mV are illustrated with fast (left-hand panels) and slow (right-hand panels) time bases. The sum of two exponentials was fitted to the data points except during the initial delay, and the slow component is shown separately. The right-hand *Y*-axis indicates the availability of the Na^+ channels, obtained by referring to the equilibrium amplitude (dotted line). *D* shows the delay time of inactivation obtained from the intersection of the exponential curve.

averaging five to twenty currents at the test potential before recording each family of current recordings.

The delayed onset of inactivation was a consistent finding at −10 mV (Fig. 3) or at more positive potentials, and suggests that inactivation does depend on activation. The above findings, however, do not necessarily exclude the possibility of inactivation directly from the closed states, since the channels may rapidly open by depolarization before the closed channels inactivate. Therefore we tested whether the delay was observed at more negative potentials where activation is slow and small. In Fig. 4, the availability tests at membrane potentials of −40 (*A*), −30 (*B*) and −20 mV (*C*) are shown. After an initial delay, the decay of availability was fitted by the sum of two exponentials. The reference level for the slow component was defined by the amplitude of the Na^+ current recorded after a long conditioning pulse. The initial delay of inactivation became longer with more negative membrane potentials during the conditioning pulse. The delay was defined for convenience by the intersection of the fitted curve with the horizontal line of maximum amplitude. The delay thus obtained was plotted against the conditioning potentials in Fig. 4*D*. It is evident that the delay was shortened as the activation process was accelerated with

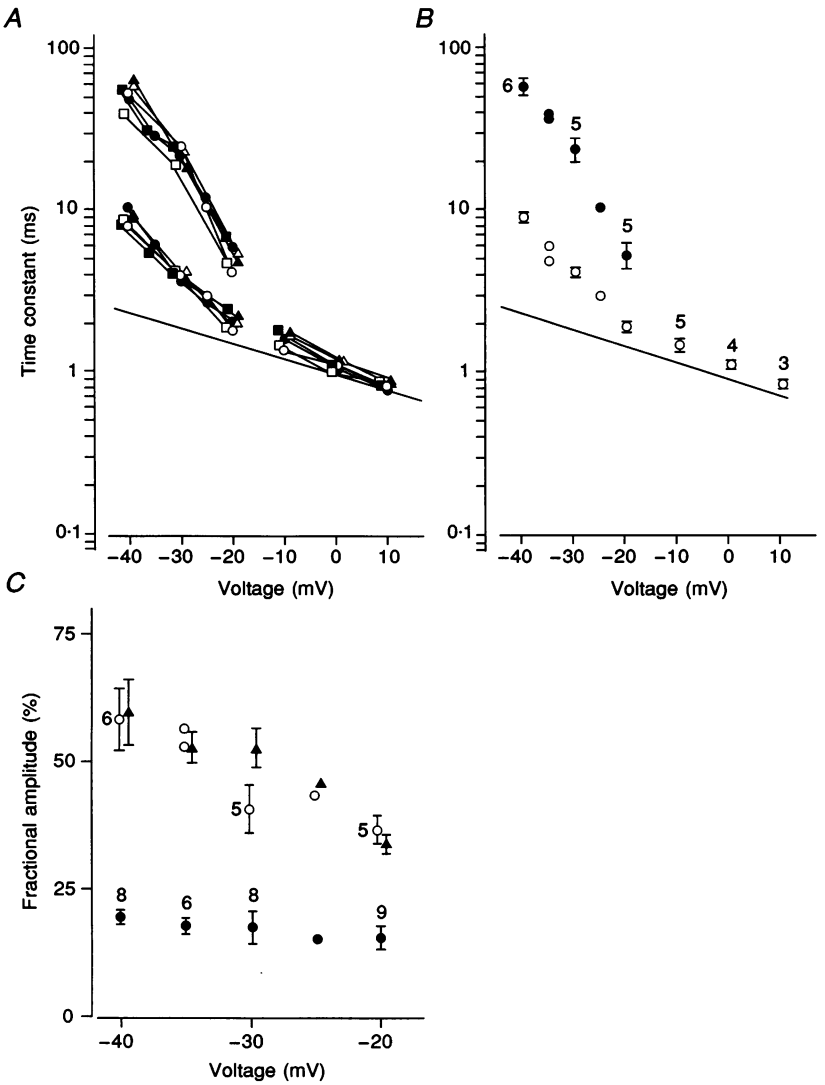

Figure 5. Time constants of inactivation

A, comparison of the time constants of the current decay (filled symbols) in the single-pulse protocol with those of availability change (open symbols) in the double-pulse protocol in three cells. Different symbols indicate different experiments. The asymptotic line determined in Fig. 2 is shown for reference in *A* and *B*. *B*, time constants (means ± S.D.) of the exponential reduction of availability, with number of experiments. *C*, fractional amplitudes (means ± S.D.) of the slow component measured from the current decay (●) or from the reduction of availability (○) determined by eqn (6). ▲, values obtained from eqn (7).

stronger depolarization. This finding is consistent with the idea of inactivation through open states.

Inactivation rates measured by the double-pulse protocol

In three experiments, the time constants of the exponential decrease of availability in the double-pulse protocol (○, △ and □) were successfully compared directly with those of the current decay in the single-pulse protocol (●, ▲ and ■) in the same cell (Fig. 5*A*). Different symbols indicate different experiments. At potentials more positive than +5 mV, the envelope of the time course was well fitted with a single exponential (Fig. 3), except for the initial delay as in the single-pulse inactivation (Fig. 1). It is evident that the values of the inactivation time constants are quite consistent, irrespective of whether they were measured from the current decay or from availability. This notion was examined by plotting the average of the time constants in the double-pulse protocol in Fig. 5*B*. These values are not significantly different from those obtained from the current decay at all potentials tested, as examined using a t test ($P < 0{\cdot}05$) for each exponential component.

Although the time constants of current decay measured by the single-pulse protocols were almost equal to those of the availability decay obtained by the double-pulse protocol, there was a significant difference in the fractional amplitude of the two exponential components as shown in Fig. 5*C*. The fractional amplitude of the slow component (●) in the current decay was always about 20% of the total, while the slow component of the availability (○) in the double-pulse protocol was larger and increased with more negative potentials over the potential range tested. This discrepancy in the fractional amplitude is explained later.

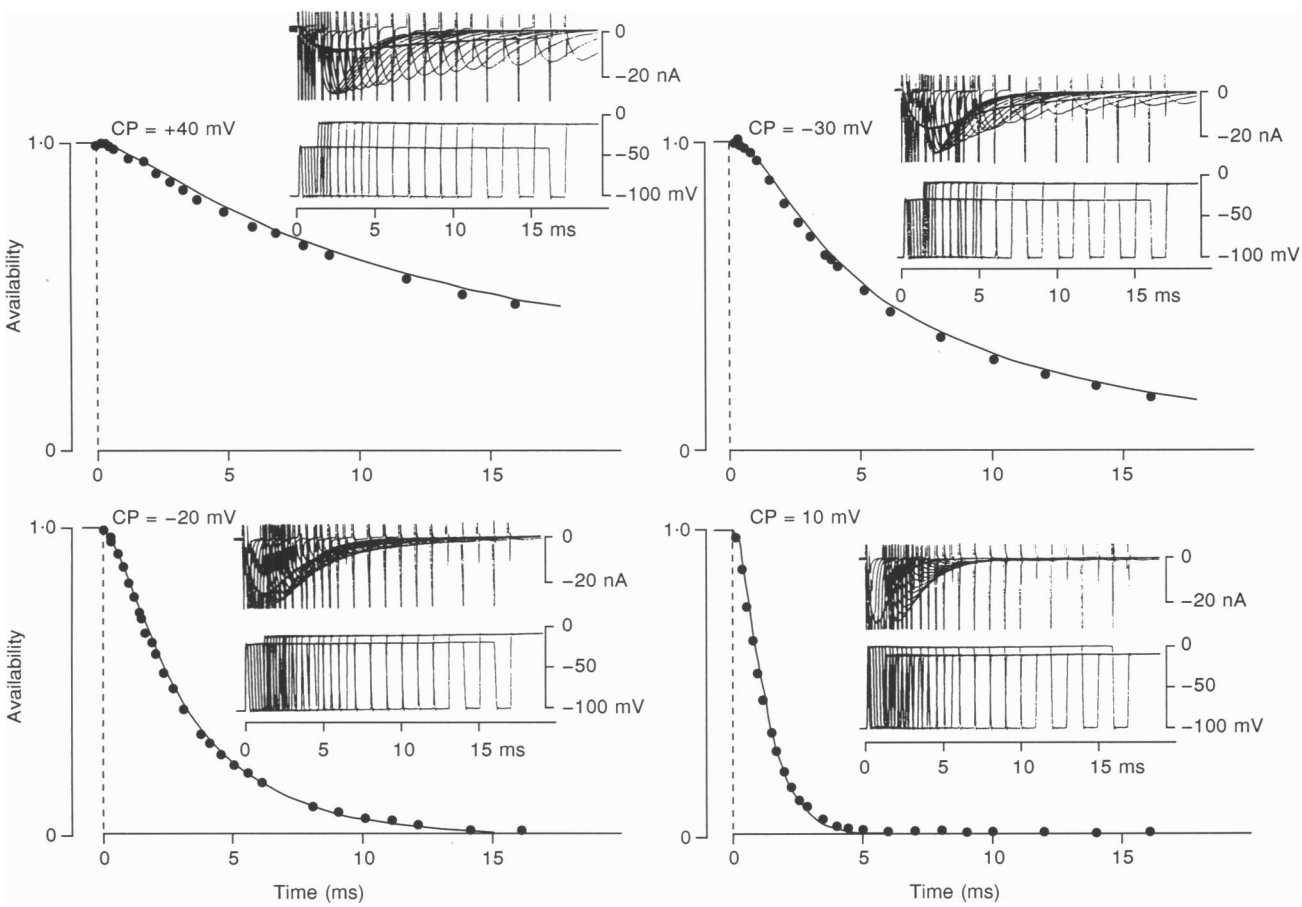

Figure 6. The normalized time integral of the Na^+ current ($1 - N_I(t)/N_I(\infty)$) superimposed onto the time course of the availability measured by the double-pulse protocol (●)

The time on the abscissa is either the duration of the conditioning pulse or the time after the onset of a continuous depolarization. Vertical interrupted lines indicate the onset of depolarization. The voltages of the conditioning pulse (CP) are indicated. The insets show superimposed membrane current and potential recordings. The potential was measured using an intracellular microelectrode in this particular experiment. The effective series resistance was obtained by plotting the deviation of the membrane potential from the command pulse (−10 mV) against the amplitude of current as in a previous study (Mitsuiye & Noma, 1992), and was 38 kΩ.

Test of inactivation exclusively through channel opening

In the present study, the Na^+ current activated by depolarization completely disappeared during the pulse. Therefore the hypothesis of inactivation exclusively through opening of the channel was tested by assuming one open state and an absorbing rate constant, β_1, for the transition from the open state to the inactivated state. The total number of inactivated Na^+ channels (N_I) is given as a function of the depolarization time (t):

$$N_I(t) = \int_0^t \beta_1 N_o(t)dt = \int_0^t \beta_1 (I_{Na}(t)/i)dt, \quad (4)$$

where $N_o(t)$ is the number of Na^+ channels in the open state at time t and i is the amplitude of the single Na^+ channel current. By normalizing $N_I(t)$ to the total number of channels inactivated ($N_I(\infty)$), we can obtain the proportion of channels in the inactivated state:

$$N_I(t)/N_I(\infty) = \int_0^t I_{Na}(t)dt / = \int_0^t I_{Na}(t)dt. \quad (5)$$

We compared the time course of $(1 - N_I(t)/N_I(\infty))$ with that of the availability ($A(t)$) measured by the double-pulse protocol as shown in Fig. 6. At every test potential the curve $(1 - N_I(t)/N_I(\infty))$ can be superimposed on the time course of $A(t)$ (●). It should be noted that the delay in the reduction of the availability in the double-pulse measurement was well described by the curve $(1 - N_I(t)/N_I(\infty))$. Essentially the same results were obtained in six cells at conditioning potentials of −40 ($n = 4$), −30 ($n = 5$), −20 ($n = 4$), −10 ($n = 4$) and 0 mV ($n = 2$). These findings strongly suggest that the inactivation of the cardiac Na^+ channel develops exclusively from the open state at potentials positive to −50 mV.

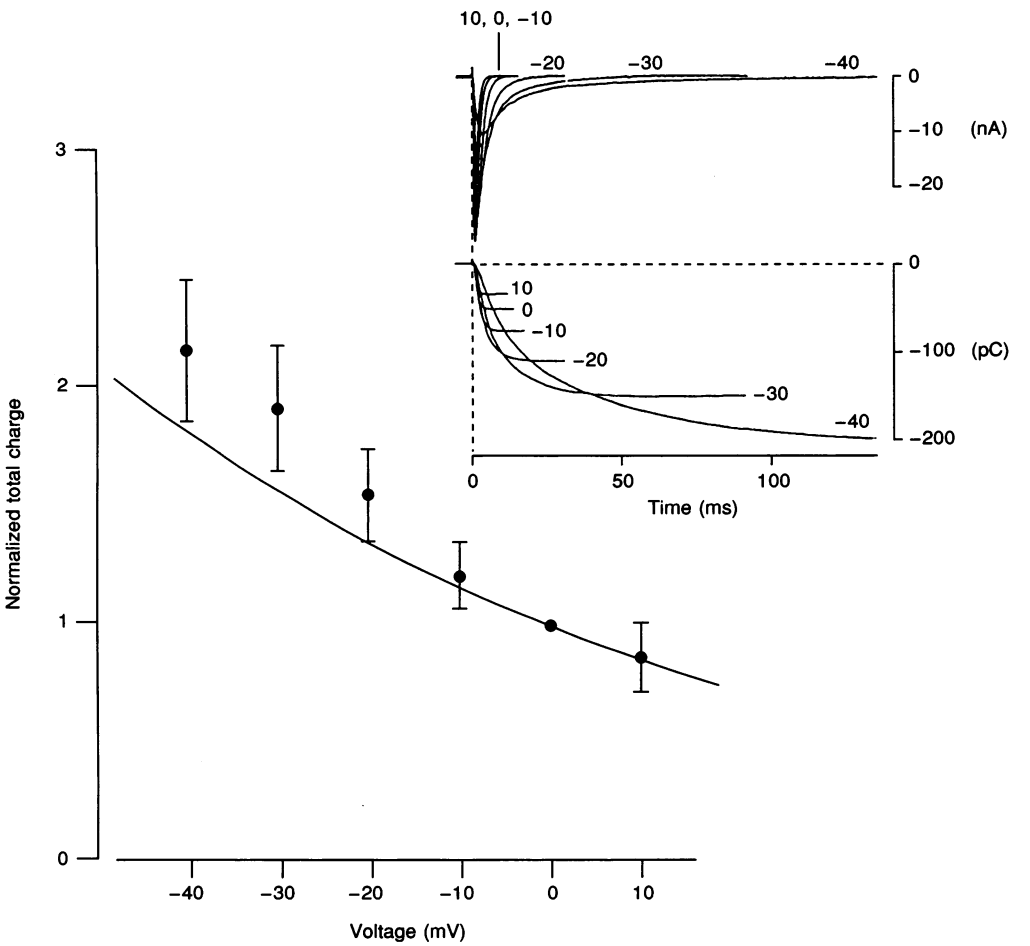

Figure 7. Relative magnitudes of the total open time determined by dividing the total charge of the whole-cell Na^+ current by the amplitude of the single Na^+ channel current

The integration of the Na^+ current at different potentials is shown in the inset. The total open times were normalized referring to the value at 0 mV, and the means ± S.D. of six experiments were plotted. The theoretical curve was drawn using eqns (11) and (13).

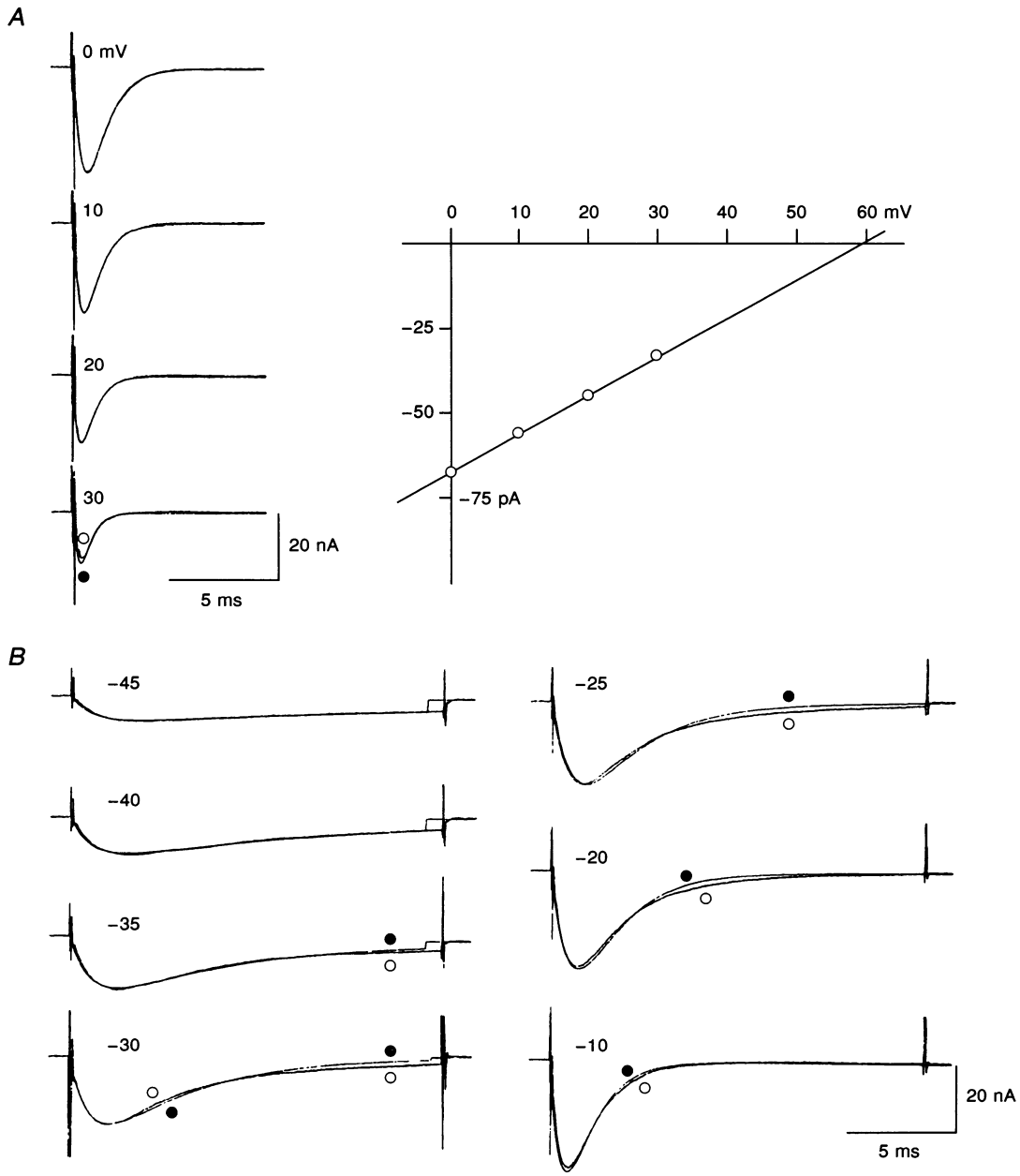

Figure 8. Fitting of Scheme (1) to the Na^+ current recordings

α_m and β_m (rate constants for the rate-limiting activation step between a closed state and an open state, respectively) were obtained by analysing Na^+ current recorded after treatment with *N*-bromoacetamide (NBA) using the same cell as in the previous study (Mitsuiye & Noma, 1993). The fitted curves are superimposed on the original currents recorded by depolarizing the membrane to the potentials indicated. The original currents and the fitted curves are indicated by ○ and ●, respectively. *A*, the Na^+ currents at positive potentials were fitted to the model with free parameters of β_i and I_{Na}. The amplitudes of $\bar{I}_{Na}$ are plotted against the membrane potential (V_m) in the right-hand graph, and this limiting conductance was used in the least-squares fit of the current at more negative potentials indicated in *B*. *B*, the Na^+ current was fitted to the model by a free parameter of β_i.

Voltage dependence of the total charge of Na^+ current

Inactivation directly from closed states was suggested by integrating the open times through the depolarizing pulse (Makielski, Sheets, Hanck, January & Fozzard, 1987). The total open time was small at positive potentials and increased with more negative potentials because the rate of inactivation became slower. With more negative potentials near the apparent threshold of activation, however, the total open time became smaller. This decrease was explained by assuming an inactivation of the Na^+ channel directly from the closed state before the channels were activated, since those channels that inactivate directly from a closed state cannot contribute to the integrated open time. To test this possibility, the Na^+ current was integrated during the pulse (Fig. 7, inset), and the total open time (D) was calculated by dividing the total charge by i, which was obtained by assuming a 20 pS single-channel conductance and a reversal potential of +60 mV. The value thus obtained gives a product $N \times D(V)$, where N is the number of channels and $D(V)$ is the total open time of a single Na^+ channel at a membrane potential of V. The value of ND thus obtained is normalized by its value at 0 mV, and the average values are plotted against potential in Fig. 7 ($n = 6$). It is evident that the total open time increases as the potential becomes more negative over the potential range examined. The result is different from the previous study (Makielski *et al.* 1987).

Apparent discrepancy in the fractional amplitude of exponential components between the single- and double-pulse protocols

Although the time constants of the current decay and the availability change were superimposable, the fractional amplitudes of the fast and slow components differed between the single-pulse and double-pulse experiments (Fig. 5*C*). We tested whether the hypothesis of inactivation exclusively through the open state can explain this discrepancy.

The double exponential curve fitted to the Na^+ current decay can be described as:

$$I_{Na}(t) = \bar{I}_{Na}((1 - S)\exp(-t/\tau_f) + S\exp(-t/\tau_s)), \quad (6)$$

where $\bar{I}_{Na}$ is the limiting amplitude of the Na^+ current and τ_f and τ_s are the time constants of the fast and the slow components, respectively. Since the delay of inactivation before the peak of activation was negligibly short compared with the decay time course, eqn (6) was used to approximate $I_{Na}(t)$ in eqn (5):

$$1 - \frac{N_I(t)}{N_I(\infty)} = \left(\frac{(1-S)\tau_f}{(1-S)\tau_f + S\tau_s}\right)\exp\left(\frac{-t}{\tau_f}\right) + \left(\frac{S\tau_s}{(1-S)\tau_f + S\tau_s}\right)\exp\left(\frac{-t}{\tau_f}\right). \quad (7)$$

Thus the fractional amplitude of the slow component of the availability measured by the double-pulse protocol is $S\tau_s/((1 - S)\tau_f + S\tau_s)$, which is different from the fractional

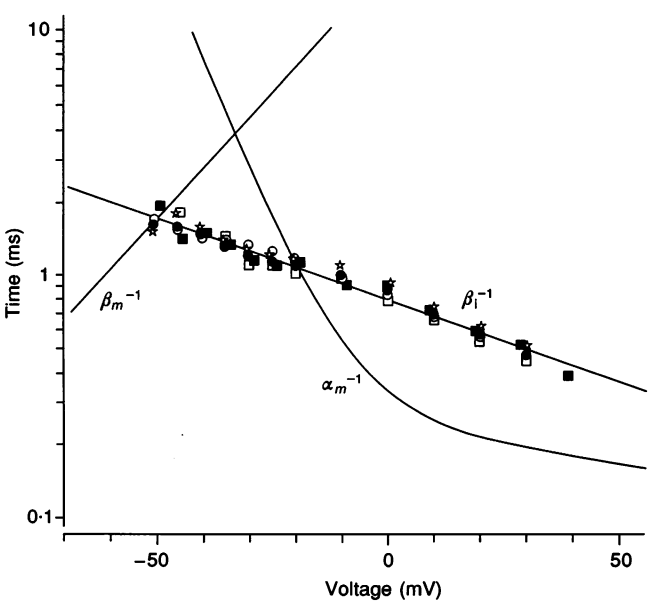

Figure 9. Semi-logarithmic plots of the reciprocal rate constants of inactivation

Different symbols indicate different experiments ($n = 5$). The line through the data points indicates eqn (11), which was obtained by using the least-squares routine. The line and the curve without data points indicate reciprocal values of α_m and β_m, calculated by eqns (9) and (10).

amplitude obtained from the single-pulse experiment. The value of $S\tau_s/((1-S)\tau_f + S\tau_s)$ was calculated from the single-pulse experiment, and its mean values are plotted in Fig. 5*C* (▲). These coincided with the experimental value obtained (○) from the double-pulse experiment. Thus the measurements are totally consistent between the two different methods.

Rate constant of inactivation from the open state

The following model is the simplest that can adequately explain the experimental findings in the present study:

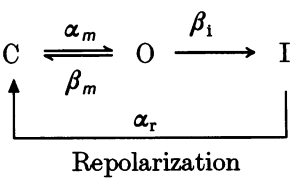

Scheme (1)

and $$I_{Na}(t) = \bar{I}_{Na} P_o(t). \quad (8)$$

where C is the closed, I is the inactivated, and O is the open state, and β_i and α_r are rate constants of inactivation and reactivation, respectively. Since inactivation is only through the open state, the time course of current decay described above (Figs 1–5 and 7) is largely affected by the activation process, especially at negative potentials. Therefore, the rate constant β_i can be determined only by fitting this scheme to $I_{Na}(t)$. Since the gating kinetics were slightly different in different experiments, both the activation and inactivation rates had to be determined in the same cell. The activation kinetics were determined for each experiment by analysing Na^+ currents recorded after *N*-bromoacetamide treatment. On average, the rate constants (s^{-1}) were:

$$\alpha_m(V) = (0{\cdot}0001027 \exp(-V/9{\cdot}3) + 0{\cdot}00025 \exp(-V/150))^{-1}, \quad (9)$$

$$\beta_m(V) = (0{\cdot}019832 \exp(V/20{\cdot}3))^{-1}, \quad (10)$$

where the membrane potential V is given in millivolts (Mitsuiye & Noma, 1993).

The experimental values of α_m and β_m were fixed in the subsequent fitting of the model leaving two free parameters of β_i and $\bar{I}_{Na}$. In Fig. 8, the original records of the Na^+ current (○) and the fitted curves (●) are shown. The fit was almost exact at positive potentials for both the activation phase and the single exponential current decay (Fig. 8*A*). The voltage relation of the limiting amplitude $\bar{I}_{Na}$ is linear, with a reversal potential of +59·5 mV in the inset of Fig. 8*A* (○). The peak amplitude of I_{Na} was 52·7 ± 1·9% ($n = 5$) of $\bar{I}_{Na}$, in accordance with the maximum open probability of about 0·57 in single-channel recordings (Kimitsuki *et al.* 1990*a*). Therefore at more negative potentials the magnitude of $\bar{I}_{Na}$ was determined from this linear relation, and was fixed in fitting the model to the Na^+ current.

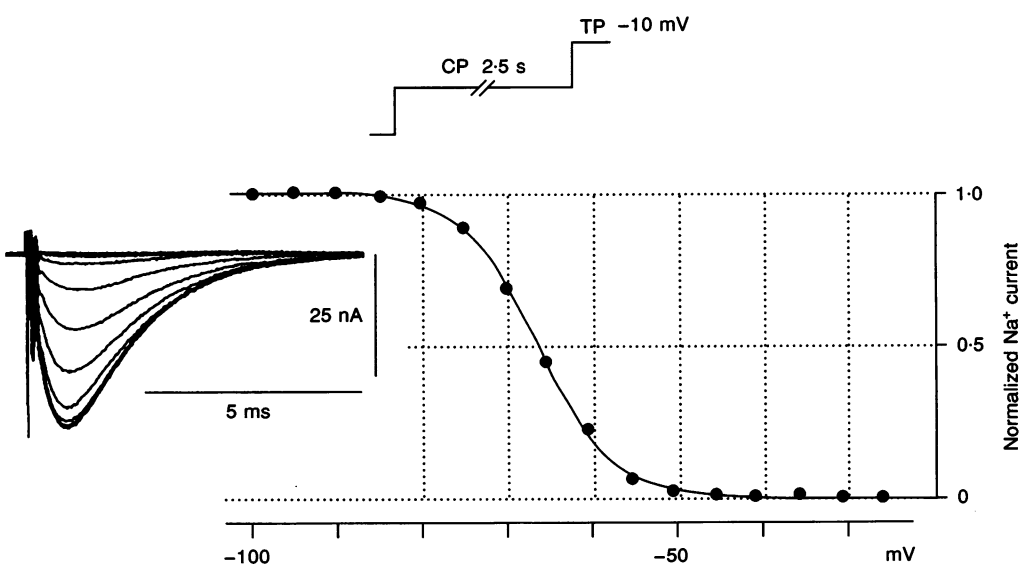

Figure 10. Measurement of the steady-state inactivation

A constant test pulse to −10 mV was applied after 2·5 s conditioning depolarizations to various levels. Peak amplitudes of the Na^+ current during the test pulse (TP) were normalized by the amplitude of the Na^+ current recorded without the conditioning pulse (CP), and are plotted against the voltage of the conditioning pulse. Note that inactivation at the physiological resting potential of −90 mV is quite small and complete inactivation is attained at potentials positive to −45 mV. The curve is the fit of the Boltzmann equation with half-inactivation of −66·5 mV and a slope factor (s) of 4·4 mV.

The reciprocal values of β_i thus determined in five experiments are plotted in Fig. 9, and were fitted with a slope of an e-fold change per 66·6 mV. Thus β_i was determined as:

$$\beta_i = (0{\cdot}000832 \exp(-V/66{\cdot}57))^{-1}. \quad (11)$$

The line and the curve without data points indicate reciprocal values of α_m; β_m is calculated by eqns (9) and (10). At negative potentials, β_i^{-1} is much smaller than the time constants of the fast and slow components of current decay shown in Fig. 2.

Measurements of steady-state inactivation

The inactivation kinetics examined above only cover potentials positive to −50 mV, where the activation of the Na^+ current was clearly resolved by the oil-gap voltage clamp. In this potential range, the steady Na^+ current was zero (Fig. 1), suggesting an absorbing inactivation. This view was consistent with measurements of steady-state inactivation $h(\infty)$. In the experiment shown in Fig. 10, a constant test pulse to −10 mV was applied following a 2·5 s conditioning depolarization to various levels without a gap between the two pulses. When the conditioning pulse potential was negative to −40 mV, the measured availability without using a gap was the same as that with a gap (not shown), and the time course of the Na^+ current activation was not obviously changed with different conditioning pulses, as shown in the inset. The peak amplitude of the Na^+ current during test pulses was normalized to that recorded without the conditioning depolarization and plotted against the voltage of the conditioning pulse. It is obvious that inactivation at the physiological resting potential is quite small, and that complete inactivation is attained at potentials positive to −45 mV. The curve superimposed is a fit of the Boltzmann equation:

$$h(\infty) = 1/(1 + \exp((V - V_{½})/s)). \quad (12)$$

In an average of five experiments, $V_{½}$ and s were −64·9 ± 1·4 and 4·4 ± 0·1 mV, respectively.

DISCUSSION

Inactivation through the open state

Measurement of Na^+ channel availability using the double-pulse protocol revealed a delayed onset of inactivation of the cardiac Na^+ channel at potentials where activation of the current was observed (Figs 3 and 4). The initial delay was well represented by calculating the time integral of I_{Na} (t) in Fig. 6, based on the gating model of Scheme (1). It is strongly suggested that the cardiac Na^+ channel inactivates exclusively from the open state, and that the inactivation step is absorbing. In general, the delayed onset of inactivation does not necessarily exclude the possibility of inactivation directly from closed states. For example, in multiple closed state models, inactivation from a closed state, which is in close proximity to the final open state, produces a delayed inactivation. However, this mechanism cannot be applied to the cardiac Na^+ channel, since activation of the Na^+ current followed a single exponential, suggesting only one rate-limiting step for Na^+ channel activation (Mitsuiye & Noma, 1992, 1993).

The hypothesis of inactivation exclusively through the open state was also supported by the fact that it explained the difference in the fractional amplitudes of the fast and slow components found in the single-pulse and the double-pulse protocols using model (1) (Fig. 5*C*). Furthermore, using rate constants in eqns (9)–(11), the total open time in Scheme (1) was calculated. The total open time (D) during depolarization to a given potential is:

$$D = \sum_{n=1}^{\infty} n\tau_o P_{OC}^{n-1}(1 - P_{OC}) = \frac{\tau_o}{1 - P_{OC}} = \frac{1}{\beta_i}, \quad (13)$$

where the probability of transition from the open state to the closed state, P_{OC}, and the mean open time, τ_o, are given as:

$$P_{OC} = \beta_m/(\beta_m + \beta_i), \quad (14)$$

$$\tau_o = 1/(\beta_m + \beta_i). \quad (15)$$

The total open time thus calculated is normalized with respect to its value at 0 mV and is shown by the curve in Fig. 7. The theoretical total open time increases with hyperpolarization and agrees well with the experimental measurements. We conclude that the gating model represented by Scheme (1) is appropriate to describe the cardiac Na^+ channel at potentials where Na^+ current activation occurs.

Comparison of the present model with the Hodgkin–Huxley-type independent model

The inactivation kinetics studied here cover only the potentials at which Na^+ current activation is obvious. At more negative potentials, the Na^+ channel inactivates without obvious macroscopic Na^+ current activation, and the inactivation step is not absorbing (Fig. 10). It might be assumed that the Na^+ channels are still inactivated at negative potentials via openings, which occur briefly and less frequently. In the model presented by Scheme (1), the steady-state fraction of I is given as:

$$I = \frac{\beta_i \dfrac{\alpha_m}{\alpha_m + \beta_m + \beta_i}}{\beta_i \dfrac{\alpha_m}{\alpha_m + \beta_m + \beta_i} + \alpha_r}. \quad (16)$$

If β_i is much smaller than $\beta_m + \alpha_m$ this equation is reduced to:

$$I = \frac{\beta_i\, m(\infty)}{\beta_i\, m(\infty) + \alpha_r}, \quad (17)$$

where $$m(\infty) = \alpha_m/(\alpha_m + \beta_m), \quad (18)$$

where $m(\infty)$ is the degree of steady-state activation.

Therefore at potentials more negative than −50 mV ($\beta_i \ll (\beta_m + \alpha_m)$), the inactivation kinetics can be reduced to first-order kinetics between one available state (Av) and one inactivated state (I), like the *h*-gate of the Hodgkin–Huxley-type model (Hodgkin & Huxley, 1952):

$$\mathrm{Av} \underset{\alpha_r}{\overset{\beta_h}{\rightleftharpoons}} \mathrm{I}, \qquad \text{Scheme (2)}$$

$$\beta_h = \beta_i\, m(\infty). \qquad (19)$$

In fact at potentials where inactivation is incomplete, the distribution of channels between the closed and open states may occur very rapidly, while transitions between the available and inactivated state occur with time constants of more than 100 ms (Follmer, Ten Eick & Yeh, 1987; Mitsuiye & Noma, 1990). The value of β_h when calculated from eqn (19) is 3·37 s^{-1} at −64·9 mV, a potential of half-availability in the steady state (Fig. 10) and is the largest time constant of the inactivation. Since the value of α_r is presumed to be the same as β_h, the expected value of τ_h is 148 ms, which is comparable to the time constant of inactivation around the potential of half-inactivation in previous studies (Follmer *et al.* 1987; Mitsuiye & Noma, 1990). Thus the experimental data in the negative potential range do not discriminate between the Hodgkin–Huxley-type independent model and the dependent model proposed by the present study.

Discrepancies from single-channel studies

Inactivation of Na^+ channels directly from the closed state was suggested mainly from single channel experiments, where a significant number (more than 30%) of sweeps in the single-channel recordings showed no channel openings, and the occurrence of null sweeps increased when activation became slower at more negative potentials. These blank sweeps were attributed to inactivation from closed states before opening of the channel (Kunze, Lacerda, Wilson & Brown, 1985; Berman *et al.* 1989; Yue *et al.* 1989; Scanley *et al.* 1990). Furthermore, Scanley *et al.* (1990) applied a five-state Markovian kinetic model to the single-channel recordings and obtained a relatively small rate constant of inactivation from the open state (50 ± 90 and 130 ± 110 s^{-1} at −57 and −52 mV, respectively), and suggested predominant inactivation from a closed state. Similarly, Yue *et al.* (1989; see the scheme in Fig. 3 in their paper), based on the results of their convolution analysis, proposed a model of the cardiac Na^+ channel where the transition rate for inactivation from a closed state is significantly higher than that of inactivation from an open state over the range of potentials of channel activation. These authors obtained a voltage dependence of inactivation from the open state which was much steeper (an e-fold change per 28 mV; calculated from the 0·9 equivalent electron charge they described) than that obtained in the present study (an e-fold change per 66·6 mV). A discrepant report is that by Berman *et al.* (1989), who obtained a negligible probability for the appearance of null sweeps at potentials where activation is complete.

The present study demonstrated that the decay of $I_{Na}(t)$ is very slow near the threshold potential, and that inward Na^+ current, i.e. opening of the channels, could be detected for at least 150 ms of depolarization to −40 mV (Fig. 1). This finding indicates that the null opening caused by direct transition to the inactivated state from a closed state should be defined by using a long depolarizing pulse at critical negative potentials. The relatively short depolarizing pulses (shorter than 50 ms) used in previous single-channel studies (Kunze *et al.* 1985; Berman *et al.* 1989; Scanley *et al.* 1990) might have missed the delayed openings of the Na^+ channel. The alternative hypothesis of Nilius (1989) that the null openings might be due to modal transitions should be thoroughly examined in single-channel recordings.

The double exponential decay of $I_{Na}(t)$

The series resistance compensation used in the present study allowed recording of a single exponential decay of the current at potentials positive to +10 mV, in contrast to the double exponential time course of inactivation recorded without an effective series resistance compensation (see Mitsuiye & Noma, 1987*a*, 1989). The single exponential decay at positive potentials suggests a single rate constant for the transition from the open to the inactivated state. The presence of two exponential components in the inactivation time course at more negative potentials was a consistent finding in both single-pulse (Fig. 2) and double-pulse inactivation experiments (Fig. 5). The model proposed in the present study assumes an absorbing inactivation and fails to explain the double exponential inactivation at negative potentials. It may be speculated that a significant fraction of Na^+ channels had slightly different activation kinetics from the remaining channels at negative potentials. Since the decay time course of $I_{Na}(t)$ is largely dependent on activation kinetics in the present model, the decay of $I_{Na}(t)$ should be the sum of two exponential components for two populations of channels with different activation kinetics. Heterogeneous activation kinetics might be due to a voltage shift of the activation kinetics of a fraction of channels, which may occur spontaneously for unknown reasons (Follmer *et al.* 1987; Makielski *et al.* 1987; Kimitsuki *et al.* 1990*b*) or by phosphorylation (Ono, Fozzard & Hanck, 1993). It is possible that the double exponential time course can be resolved only at negative potentials where the kinetics are slow, but at positive potentials the difference in the rapid activation kinetics becomes negligible, so that the decay time course can be fitted only by single exponentials. This possibility remains to be examined.

The Na^+ current was completely inactivated at potentials less negative than −50 mV in the present study, and the slow component of exponential inactivation was successfuly defined by referring to the zero-current level. The

magnitude as well as the voltage dependence of the time constants were consistent in both the single-pulse and double-pulse measurements of inactivation. This finding is different from previous studies. Both in nerve (Goldman & Shauf, 1973; Oxford & Pooler, 1975) and in heart (Benndorf & Nilius, 1987; Mitsuiye & Noma, 1987*b*, 1989), it has been reported that the time constant of decay of the current is up to ten-fold faster than the reduction in availability measured by double-pulse experiments at negative potentials where activation is small. It might be suggested that the slow component of the Na^+ current was not clearly resolved in those studies using relatively short pulses.

Benndorf, K. & Nilius, B. (1987). Inactivation of sodium channels in isolated myocardiac mouse cells. *European Biophysics Journal* **15**, 117–127.

Berman, M. F., Camardo, J. S., Robinson, R. B. & Siegelbaum, S. A. (1989). Single sodium channels from canine ventricular myocytes: voltage dependence and relative rates of activation and inactivation. *Journal of Physiology* **415**, 503–531.

Bezanilla, F. A. & Armstrong, C. M. N. (1977). Inactivation of the sodium channel. I. Sodium current experiments. *Journal of General Physiology* **70**, 549–566.

Colquhoun, D. (1971). *Lectures on Biostatics.* Clarendon Press, Oxford.

Follmer, C. H., Ten Eick, R. E. & Yeh, J. Z. (1987). Sodium current kinetics in cat atrial myocytes. *Journal of Physiology* **384**, 169–197.

Gillespie, J. I. & Meves, H. (1980). The time course of sodium inactivation in squid giant axons. *Journal of Physiology* **299**, 289–308.

Goldman, L. & Kenyon, J. L. (1982). Delays in inactivation development and activation kinetics in *Myxicola* giant axons. *Journal of General Physiology* **80**, 83–102.

Goldman, L. & Shauf, C. L. (1973). Quantitative description of sodium and potassium currents and computed action potentials in *Myxicola* giant axons. *Journal of General Physiology* **61**, 361–384.

Hodgkin, A. L. & Huxley, A. F. (1952). A quantitative description of membrane current and its application to conductance and excitation in nerve. *Journal of Physiology* **117**, 500–544.

Isenberg, G. & Klöckner, U. (1982). Calcium tolerant ventricular myocytes prepared by preincubation in a "KB medium". *Pflügers Archiv* **395**, 6–18.

Kimitsuki, T., Mitsuiye, T. & Noma, A. (1990*a*). Maximum open probability of single Na^+ channels during depolarization in guinea-pig cardiac cells. *Pflügers Archiv* **416**, 493–500.

Kimitsuki, T., Mitsuiye, T. & Noma, A. (1990*b*). Negative shift of cardiac Na^+ channel kinetics in cell-attached patch recordings. *American Journal of Physiology* **258**, H247–254.

Kunze, D. J., Lacerda, A. E., Wilson, D. L. & Brown, A. M. (1985). Cardiac Na^+ current and the inactivating, reopening and waiting properties of single cardiac Na^+ channels. *Journal of General Physiology* **86**, 691–719.

Makielski, J. C., Sheets, M. F., Hanck, D. A., January, C. T. & Fozzard, H. A. (1987). Sodium current in voltage clamped internally perfused canine Purkinje cells. *Biophysical Journal* **52**, 1–11.

Mitsuiye, T. & Noma, A. (1987*a*). A new oil-gap method for internal perfusion and voltage clamp of single cardiac cells. *Pflügers Archiv* **410**, 7–14.

Mitsuiye, T. & Noma, A. (1987*b*). Inactivation of guinea-pig cardiac Na^+ current as examined by the new oil-gap method. *Journal of Physiology* **394**, 42*P*.

Mitsuiye, T. & Noma, A. (1989). Kinetics of sodium current inactivation in cardiac ventricular cell of guinea-pig studied by the oil-gap voltage clamp. *Current Topics in Antiarrhythmic Agents, Current Clinical Practice Series*, vol. 56, pp. 3–14. Excerpta Medica, Tokyo.

Mitsuiye, T. & Noma, A. (1992). Exponential activation of the cardiac Na^+ current in single guinea-pig ventricular cells. *Journal of Physiology* **453**, 261–277

Mitsuiye, T. & Noma, A. (1993). Quantification of the exponential activation of the cardiac Na^+ current in *N*-bromoacetamide-treated cardiac myocytes of guinea-pig. *Journal of Physiology* **465**, 245–263.

Nilius, B. (1988). Modal gating behaviour of cardiac sodium channels in cell-free membrane patches. *Biophysical Journal* **53**, 857–862.

Nonner, W. (1980). Relations between the inactivation of sodium channels and the immobilization of gating charge in frog myelinated nerve. *Journal of Physiology* **299**, 573–603.

Ono, K., Fozzard, H. A. & Hanck, D. A. (1993). Mechanism of cAMP-dependent modulation of cardiac sodium channel current kinetics. *Circulation Research* **72**, 807–815.

Oxford, G. S. & Pooler, J. P. (1975). Selective modification of sodium channel gating in lobster axons by 2,4,6-trinitrophenol. Evidence for two inactivation mechanisms. *Journal of General Physiology* **66**, 765–780.

Powell, T., Terrar, D. A. & Twist, V. W. (1980). Electrical properties of individual cells isolated from adult rat myocardium. *Journal of Physiology* **302**, 131–153.

Scanley, B. E., Hanck, D. A., Chay, T. & Fozzard, H. A. (1990). Kinetic analysis of single sodium channels from canine cardiac Purkinje cells. *Journal of General Physiology* **95**, 411–437.

Yue, D. T., Lawrence, J. H. & Marban, E. (1989). Two molecular transitions influence cardiac sodium channel gating. *Science* **244**, 349–352.

Acknowledgements

This work was supported by Grants in Aid for Scientific Research from the Ministry of Education, Science and Culture of Japan.

Received 12 August 1994; accepted 15 December 1994.